analytical chemistry

pubs.acs.org/ac

Article

Evaluation of the Higher Order Structure of Biotherapeutics Embedded in Hydrogels for Bioprinting and Drug Release

Domenico Rizzo, Linda Cerofolini, Anna Pérez-Ràfols, Stefano Giuntini, Fabio Baroni, Enrico Ravera, Claudio Luchinat, and Marco Fragai*

Cite This: *Anal. Chem.* 2021, 93, 11208–11214

Read Online

ACCESS | Metrics & More | Article Recommendations | Supporting Information

ABSTRACT: Biocompatible hydrogels for tissue regeneration/replacement and drug release with specific architectures can be obtained by three-dimensional bioprinting techniques. The preservation of the higher order structure of the proteins embedded in the hydrogels as drugs or modulators is critical for their biological activity. Solution nuclear magnetic resonance (NMR) experiments are currently used to investigate the higher order structure of biotherapeutics in comparability, similarity, and stability studies. However, the size of pores in the gel, protein−matrix interactions, and the size of the embedded proteins often prevent the use of this methodology. The recent advancements of solid-state NMR allow for the comparison of the higher order structure of the matrix-embedded and free isotopically enriched proteins, allowing for the evaluation of the functionality of the material in several steps of hydrogel development. Moreover, the structural information at atomic detail on the matrix−protein interactions paves the way for a structure-based design of these biomaterials.

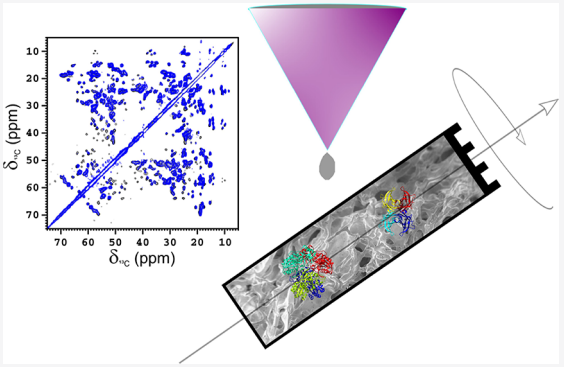

INTRODUCTION

The continuous development of new biocompatible materials is opening new frontiers in medicine and new biotechnological opportunities. Several biomaterials are currently used to replace/support non-functional tissues like those damaged or destroyed by injuries or diseases and in controlled drug release. Materials for tissue regeneration are designed to provide mechanical support to the surrounding tissue, to stimulate cell growth, and to modulate the immune response promoting an extensive cell colonization and matrix reabsorption.[1,2] Composite scaffolds with a highly resolved architecture, incorporating proteins and seeding cells, can be obtained by three-dimensional (3D) bioprinting techniques starting from biocompatible hydrogels like those formed by hyaluronic acid[3−7] or mixtures of alginate and gelatine.[6,8−13] In this context, there is an increasing interest in loading proteins on hydrogels as drugs or modulators of the biological activity.[14−25] The biological function of a protein is strictly related to its native folding, and the preservation of the higher order structure (HOS) in the composite biomaterial is crucial for its therapeutic function. Actually, the interaction of the protein with the matrix components can alter the protein structure leading to a loss of activity and immunological effects.

Several biophysical methodologies, such as attenuated total reflectance Fourier-transformed infrared and fluorescence spectroscopy, circular dichroism, and differential scanning calorimetry, are usually used to characterize the protein component in heterogeneous materials.[26−28] However, these analytical methods measure different aspects of the structure, either directly or indirectly, and are often not sensitive enough to small, local changes in the protein fold. Nuclear magnetic resonance (NMR) and mass spectrometry are well-established techniques to investigate the preservation of the HOS of biologics in solution.[29−39] Solution NMR has been used previously on small proteins and peptides embedded in hydrogels to investigate the folding state in a confined environment[40] and for the structural characterization through residual dipolar couplings, since hydrogels behave as anisotropic external alignment media.[41−43] However, when the size of the pores in the gels is too small or strong interactions between the gel matrix and the cargo protein take place, the rotational correlation time of the protein in solution increases and makes solution NMR ineffective in the analysis of the protein structure at the atomic level.

Recently, solid-state NMR has emerged as a tool to characterize the protein component and to reveal protein−matrix interactions in heterogeneous materials. In this respect,

Received: April 30, 2021
Accepted: July 20, 2021
Published: August 2, 2021

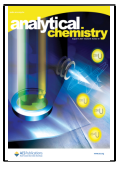

https://doi.org/10.1021/acs.analchem.1c01850
Anal. Chem. 2021, 93, 11208−11214

the use of solid-state NMR has been described to characterize noncrystalline large protein assemblies,[44−50] biomaterials,[51,52] bioinspired silica matrix embedding enzymes,[53−58] conjugated proteins,[59−62] protein-grafted nanoparticles,[63] and vaccines.[64−66] Here, we prove that solid-state NMR provides detailed information on the preservation of the HOS of proteins embedded into two popular matrices used for 3D bioprinting.

The therapeutic protein *E. coli* asparaginase-II (ANSII), clinically used against acute lymphoblastic leukemia, has recently shown its activity also against solid tumor when administered in long half-life formulations that reduce immunological adverse reactions.[67]

Human transthyretin (TTR) is a physiological protein acting as a hormone carrier.[68,69] Although some genetic variants of TTR lead to a systemic amyloidosis called familial amyloid polyneuropathy,[70] TTR is a potential drug carrier and has been recently proposed as a multivalency Fab platform for target clustering.[71]

Therefore, these two proteins are suitable models to investigate how the matrices used for 3D bioprinting interplay with embedded proteins and are used here to prove the potential of solid-state NMR (SSNMR) in the characterization of the protein components during the design of these composite hydrogels.

EXPERIMENTAL SECTION

Sample Preparation and NMR Measurements. [U-^{13}C-^{15}N] ANSII was expressed and purified as previously described.[59,61−64] The expression and purification protocol of [U-^{13}C-^{15}N] TTR is reported in the Supporting Information. All the hydrogels embedding the selected proteins (ANSII and TTR) were directly generated in Bruker 3.2 mm thin-walls zirconia rotors with bottom and top caps, starting from the dried materials prepared by using the different procedures described below.

The sample of [U-^{13}C-^{15}N] ANSII encapsulated in the alginate/gelatine hydrogel was prepared by incorporating the freeze-dried protein (4 mg) into a mixture of 1:1 alginate/gelatine powders (5 mg) and then by rehydrating the dried mixture within the rotor.[72] A different procedure was used to prepare the sample of [U-^{13}C-^{15}N] TTR encapsulated in the alginate/gelatine hydrogel. The dry mixture containing TTR was prepared by lyophilizing a solution containing all the components (6 mg of protein and 5 mg of the 1:1 alginate/gelatine mixture). In both cases, the dried material was packed in the rotor and hydrated with MilliQ H_2O to reach a final concentration of ∼5−7% w/w for alginate and gelatine. Finally, a concentrated solution of $CaCl_2$ (to reach a concentration of 100 mM in the rotor) was added to cross-link the hydrogel materials within the rotor.[73,74]

A sample of [U-^{13}C-^{15}N] TTR protein encapsulated in the alginate/gelatine hydrogel was also analyzed by solution NMR. The gel was prepared by dissolving a mixture of alginate and gelatine (∼7% w/w) in 600 μL of a solution of TTR (100 μM in 50 mM MES, pH 6.5, 100 mM NaCl, 5 mM DTT). Then, the material was transferred in a 5 mm tube and cross-linked by adding a concentrated solution of $CaCl_2$ (to reach a concentration of 100 mM) in the NMR tube. The 2D ^{1}H-^{15}N TROSY-HSQC spectrum recorded on the encapsulated protein was superimposed with that of TTR collected in solution (see Figure S1).

The hyaluronic acid hydrogels encapsulating the selected proteins ([U-^{13}C-^{15}N] ANSII or TTR) were prepared by packing the rotor with consecutive layers of the freeze-dried protein (∼4−6 mg) and freeze-dried hyaluronic acid (Jonexa, 7−9 mg), which had been previously dialyzed against MilliQ H_2O to remove the excess of salts. The material was finally rehydrated with MilliQ H_2O (from 10 to 20 μL). Sample homogeneity was obtained after rotor spinning and supported by the quality of the spectra that suggests the presence of a protein experiencing a single environment.

Samples of freeze-dried proteins were prepared as reference. The free proteins (∼20 and 25 mg of ANSII and TTR, respectively) were freeze-dried in the presence of PEG1000 (4 and 2.5 mg for ANSII and TTR, respectively); the materials were packed into a Bruker 3.2 mm zirconia rotor and rehydrated with MilliQ H_2O (∼9 and 16 μL for ANSII and TTR, respectively). $CaCl_2$ was not present in the samples of rehydrated freeze-dried proteins.

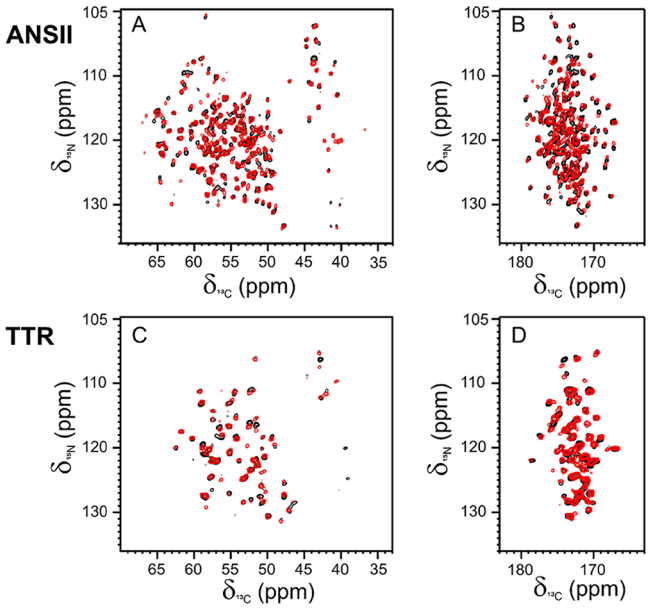

Figure 1. (A, C) 2D ^{15}N ^{13}C NCA and (B, D) NCO spectra of ANSII-HA (red, top) and TTR-HA (red, bottom) superimposed with NCA and NCO of the rehydrated freeze-dried reference proteins (black). The spectra were acquired at ∼290 K, MAS 14 kHz and 800 MHz.

Silicon plugs (courtesy of Bruker Biospin) placed below the turbine cap were used to close the rotor and preserve hydration.

SSNMR experiments were recorded on a Bruker Avance III spectrometer operating at 800 MHz (18.8 T, 201.2 MHz ^{13}C Larmor frequency) equipped with a Bruker 3.2 mm Efree NCH probe-head. The spectra were recorded at 14 kHz MAS frequency, and the sample temperature was kept at ∼290 K. The sample of the alginate/gelatine hydrogel encapsulating TTR was also investigated at a higher spinning frequency (16 and 20 kHz).

Standard ^{13}C-detected SSNMR spectra (2D ^{15}N-^{13}C NCA, ^{15}N-^{13}C NCO, and ^{13}C-^{13}C DARR, mixing time 50 ms) were acquired on all the samples (except for TTR encapsulated in the alginate/gelatine hydrogel) using the pulse sequences reported in the literature.[75] 2D ^{13}C-^{13}C CORDxy4[76] was instead recorded for the sample of the alginate/gelatine

https://doi.org/10.1021/acs.analchem.1c01850
Anal. Chem. 2021, 93, 11208−11214

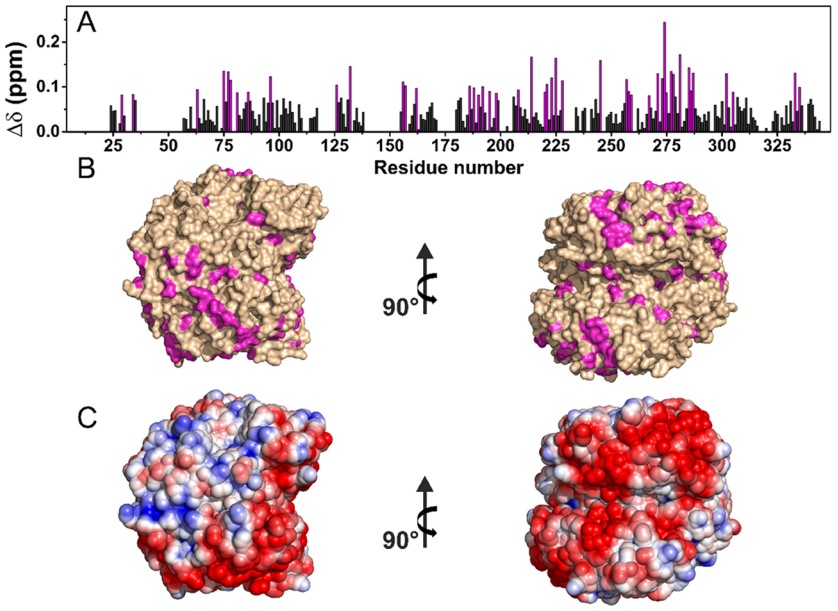

Figure 2. (A) Chemical shift perturbations (CSPs) of ANSII-HA with respect to rehydrated freeze-dried ANSII, evaluated according to the formula $\Delta\delta = \frac{1}{2}\sqrt{(\Delta\delta_{C\alpha}/2)^2 + (\Delta\delta_N/5)^2}$. The residues experiencing the largest variations have been highlighted in magenta. (B) CSP mapping on the protein surface (PDB code: 3ECA) with the region with the largest perturbation in magenta. (C) Electrostatic potential generated by APBS plugin in PyMOL on 3ECA with blue and red representing the regions of positive and negative electrostatic potential, respectively.

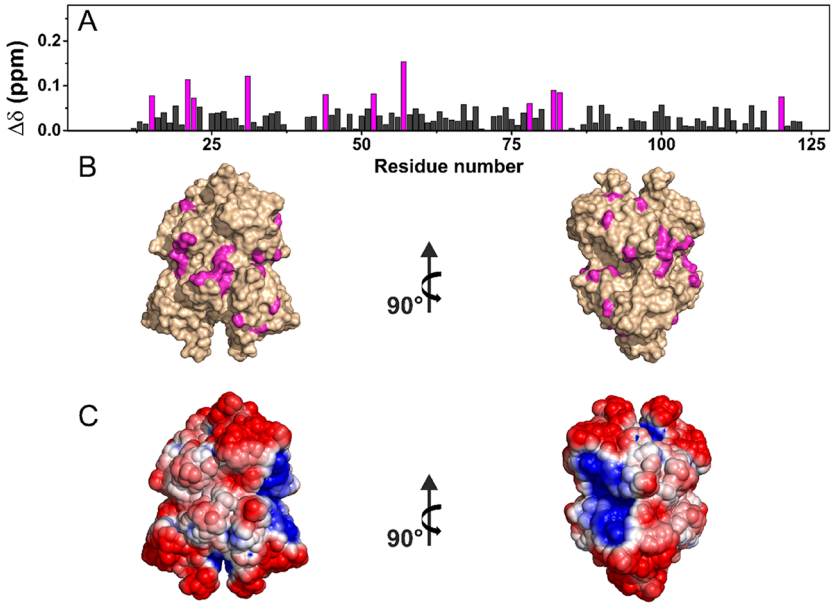

Figure 3. (A) Chemical shift perturbations (CSPs) of TTR-HA with respect to rehydrated freeze-dried TTR, evaluated according to the formula $\Delta\delta = \frac{1}{2}\sqrt{(\Delta\delta_{C\alpha}/2)^2 + (\Delta\delta_N/5)^2}$. The residues experiencing the largest variations have been highlighted in magenta. (B) CSP mapping on the protein surface (PDB code: 1BMZ) with the region with the largest perturbation in magenta. (C) Electrostatic potential generated by APBS plugin in PyMOL on 1BMZ with blue and red representing the regions of positive and negative electrostatic potential, respectively.

hydrogel encapsulating TTR at a higher frequency speed (20 kHz), to favor the protein sedimentation.

All the spectra were processed with the Bruker TopSpin 3.2 software package and analyzed with the program CARA.[77]

RESULTS AND DISCUSSION

Analysis of the Preservation of the HOS of the Proteins Encapsulated in the Hyaluronic Acid Hydrogel by SSNMR. The selected proteins (ANSII and TTR) encapsulated in the hyaluronic acid hydrogel (ANSII-HA and TTR-HA, respectively) were first analyzed by SSNMR. The 1D $\{^1H\}$-^{13}C cross polarization spectra of ANSII-HA and TTR-HA show well-resolved and sharp signals with quality comparable with that of the spectra of the rehydrated freeze-dried materials (Figure S2).

Despite the limited concentration of the embedded proteins in the hydrogel, the 2D amide-carbon alpha (2D ^{15}N ^{13}C NCA) and amide-carbonyl (2D ^{15}N ^{13}C NCO) correlation spectra of ANSII-HA (Figure 1A,B) and TTR-HA (Figure

https://doi.org/10.1021/acs.analchem.1c01850
Anal. Chem. 2021, 93, 11208−11214

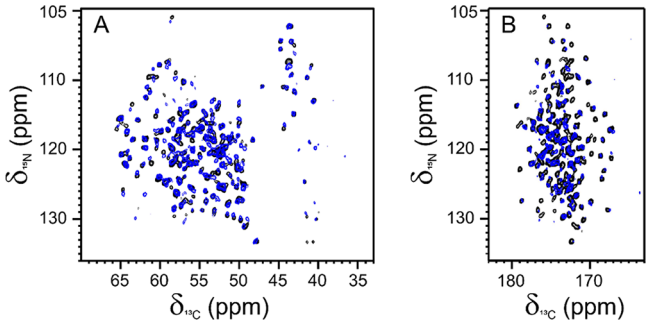

Figure 4. (A) 2D ^{15}N ^{13}C NCA and (B) NCO spectra of ANSII-AG (blue) superimposed with the NCA and NCO of the rehydrated freeze-dried reference protein (black). The spectra were acquired at ∼290 K, MAS 14 kHz and 800 MHz.

1C,D) are of high quality and comparable, for the number of cross-peaks detected, with those of rehydrated freeze-dried proteins. For both proteins embedded in the hyaluronic acid matrix, the matching of the resonances of the 2D-NMR spectral fingerprints with those of their own reference allows us to assess the preservation of the HOS after encapsulation in the matrix.

The assignment of the 2D ^{15}N ^{13}C NCA and NCO spectra of ANSII-HA and TTR-HA was easily obtained by comparison with the 2D ^{15}N ^{13}C NCA and NCO collected for the rehydrated freeze-dried proteins and also using the information from the 2D ^{13}C-^{13}C correlation spectrum (dipolar assisted rotational resonance, DARR) acquired for ANSII-HA and TTR-HA. The analyses of the chemical shift perturbation (CSP) of the NCA spectra of the proteins embedded in the hyaluronic acid hydrogels, with respect to the NCA of the corresponding rehydrated freeze-dried references, are reported in Figures 2 and 3. Most CSP values were less than 0.1 ppm for ANSII-HA and even lower for TTR-HA. The analysis of the CSPs shows that for ANSII-HA, hydrophobic (Ala, Val, Ile, Tyr, and Phe) and neutral polar (Thr, Ser, Asn, and Gln) residues experience the largest effects (Figure 2). Minimal CSPs were observed in TTR-HA protein where the largest effects again involve hydrophobic residues and neutral polar surface patches (Figure 3).

Analysis of the Preservation of the HOS of the Proteins Encapsulated in the Alginate/Gelatine Hydrogel by SSNMR. The same analysis was also performed on the alginate/gelatine hydrogels encapsulating ANSII and TTR, respectively (ANSII-AG and TTR-AG). The 1D {^{1}H}-^{13}C cross polarization spectra of ANSII-AG and TTR-AG show the same spreading of the resonances of the corresponding rehydrated freeze-dried analogue. However, in particular for TTR-AG, the signals feature broader lines than in the rehydrated freeze-dried protein (Figure S2).

The NCA and NCO correlation spectra collected for ANSII-AG (Figure 4) are still of high quality and comparable, for the number of cross-peaks detected, with those collected on rehydrated freeze-dried ANSII. On the contrary, for TTR-AG, the fast decay of the NMR signal does not allow us to collect high quality and well-resolved 2D spectra. However, by increasing the spinning rate up to 16 and 20 kHz, the signals become sharper and increase in intensity (Figure S3), indicating a more efficient protein immobilization. Therefore, it was possible to acquire a 2D ^{13}C-^{13}C correlation spectrum at 20 kHz, which allowed us to assess the folding state of the protein in the hydrogel and, after comparison with that acquired for the rehydrated freeze-dried reference (Figure S4), confirm the preservation of the HOS after encapsulation. The structural analysis of TTR encapsulated in the alginate/gelatine matrix was also attempted using solution NMR. However, all the signals, but the N- and C-termini (Thr3-Ser8; Lys126-Glu127), are broadened beyond detection (Figure S1).

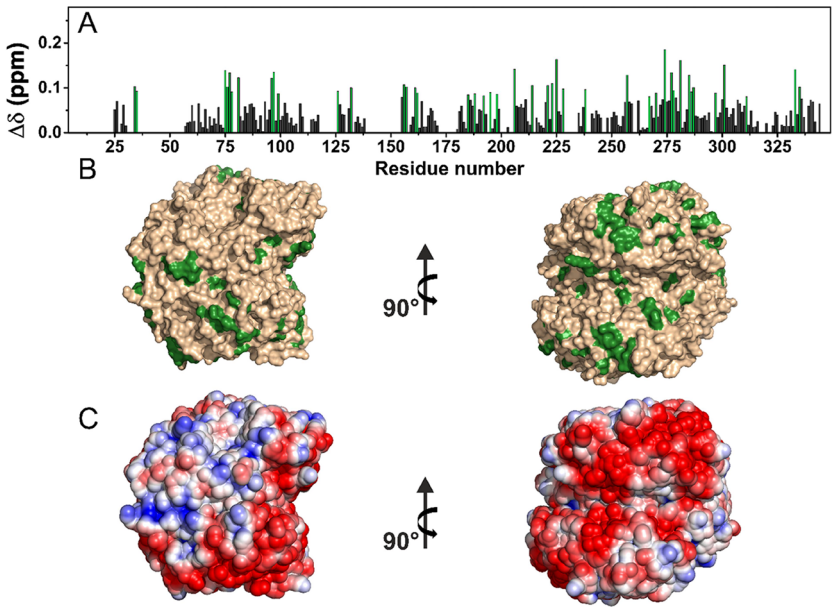

Figure 5. (A) Chemical shift perturbations (CSPs) of ANSII-AG with respect to rehydrated freeze-dried ANSII, evaluated according to the formula $\Delta\delta = \frac{1}{2}\sqrt{(\Delta\delta_{C\alpha}/2)^2 + (\Delta\delta_N/5)^2}$. The residues experiencing the largest variations have been highlighted in green. (B) CSP mapping on the protein surface (PDB code: 3ECA) with the region with the largest perturbation in green. (C) Electrostatic potential generated by APBS plugin in PyMOL on 3ECA with blue and red representing the regions of positive and negative electrostatic potential, respectively.

https://doi.org/10.1021/acs.analchem.1c01850
Anal. Chem. 2021, 93, 11208−11214

The assignment of the ANSII-AG spectra could be easily obtained by comparison with the spectra collected for the rehydrated freeze-dried protein and complemented with the information from the 2D ^{13}C-^{13}C correlation spectrum acquired for ANSII-AG. The analysis of the CSP of the NCA spectrum of ANSII-AG with respect to the NCA of the rehydrated freeze-dried reference is reported in Figure 5.

The analysis of the CSPs shows that also for ANSII-AG, hydrophobic (Ala, Val, Ile, Tyr, and Phe) and neutral polar (Thr, Ser, Ans, and Gln) residues experience the largest effects. In particular, many threonine residues are affected by significant CSP, thus suggesting a possible interaction of these surface residues with the hydroxyl groups of alginate in the hydrogel.

Collectively, the good superimposition of the spectra and the small CSPs observed for the two proteins prove the preservation of their native HOS, thus providing the first fundamental information on the investigated biomaterial. Additional information on protein−matrix interactions is obtained from the line broadening of the signals in the spectra. For TTR, the large line broadening, its dependence from the spinning rate, and the small CSPs suggest a weaker protein−matrix interaction with respect to ANSII protein, although the different molecular weights may also play a role. The different behavior is probably related to the different sizes of the proteins and to the physical−chemical properties of the surface due to the different amino acid compositions. In this respect, the observation that hydrophobic and polar neutral amino acids on the protein surface experience the largest effects provides a way to design possible chemical modifications of the matrix in order to tune the protein−matrix interactions and the properties of the resulting biomaterial.[78−82]

CONCLUSIONS

In summary, we demonstrate that 2D-SSNMR spectra can be exploited to assess the preservation of HOS of proteins when embedded in matrices used for 3D bioprinting and drug release. This analytical method can be integrated in the pipeline for the development of new composite hydrogels bearing biotherapeutics. In particular, when the assignment is available, the analysis of the residues experiencing chemical shift variations can provide information for a quality by design approach of these innovative biomaterials.

ASSOCIATED CONTENT

Supporting Information

The Supporting Information is available free of charge at https://pubs.acs.org/doi/10.1021/acs.analchem.1c01850.

Protocols for the expression and purification of isotopically enriched *E. coli* asparaginase-II (ANSII) and human transthyretin (TTR) and figures showing additional spectra of *E. coli* asparaginase-II (ANSII) and human transthyretin (TTR) (PDF)

AUTHOR INFORMATION

Corresponding Author

Marco Fragai − *Magnetic Resonance Center (CERM), University of Florence, and Consorzio Interuniversitario Risonanze Magnetiche di Metalloproteine (CIRMMP), Sesto Fiorentino 50019, Italy; Department of Chemistry "Ugo Schiff", University of Florence, Sesto Fiorentino 50019, Italy;* orcid.org/0000-0002-8440-1690; Phone: +39 055 4574261; Email: fragai@cerm.unifi.it

Authors

Domenico Rizzo − *Magnetic Resonance Center (CERM), University of Florence, and Consorzio Interuniversitario Risonanze Magnetiche di Metalloproteine (CIRMMP), Sesto Fiorentino 50019, Italy; Department of Chemistry "Ugo Schiff", University of Florence, Sesto Fiorentino 50019, Italy*

Linda Cerofolini − *Magnetic Resonance Center (CERM), University of Florence, and Consorzio Interuniversitario Risonanze Magnetiche di Metalloproteine (CIRMMP), Sesto Fiorentino 50019, Italy*

Anna Pérez-Ràfols − *Department of Chemistry "Ugo Schiff", University of Florence, Sesto Fiorentino 50019, Italy; Giotto Biotech, S.R.L, Sesto Fiorentino, Florence 50019, Italy*

Stefano Giuntini − *Magnetic Resonance Center (CERM), University of Florence, and Consorzio Interuniversitario Risonanze Magnetiche di Metalloproteine (CIRMMP), Sesto Fiorentino 50019, Italy; Department of Chemistry "Ugo Schiff", University of Florence, Sesto Fiorentino 50019, Italy*

Fabio Baroni − *Analytical Development Biotech Department, Merck Serono S.p.a, Merck KGaA, Guidonia, Rome 00012, Italy*

Enrico Ravera − *Magnetic Resonance Center (CERM), University of Florence, and Consorzio Interuniversitario Risonanze Magnetiche di Metalloproteine (CIRMMP), Sesto Fiorentino 50019, Italy; Department of Chemistry "Ugo Schiff", University of Florence, Sesto Fiorentino 50019, Italy;* orcid.org/0000-0001-7708-9208

Claudio Luchinat − *Magnetic Resonance Center (CERM), University of Florence, and Consorzio Interuniversitario Risonanze Magnetiche di Metalloproteine (CIRMMP), Sesto Fiorentino 50019, Italy; Department of Chemistry "Ugo Schiff", University of Florence, Sesto Fiorentino 50019, Italy*

Complete contact information is available at: https://pubs.acs.org/10.1021/acs.analchem.1c01850

Author Contributions

The manuscript was written through contributions of all authors. All authors have given approval to the final version of the manuscript.

Notes

The authors declare no competing financial interest.

ACKNOWLEDGMENTS

This work has been supported by Regione Toscana (CERM-TT and BioEnable), Fondazione Cassa di Risparmio di Firenze, the Italian Ministero dell'Istruzione, dell'Università e della Ricerca through PRIN 2017A2KEPL, the "Progetto Dipartimenti di Eccellenza 2018-2022" to the Department of Chemistry "Ugo Schiff" of the University of Florence, and the Recombinant Proteins JOYNLAB laboratory. The authors acknowledge the support and the use of resources of Instruct-ERIC, a landmark ESFRI project, and specifically the CERM/CIRMMP Italy centre. We acknowledge H2020 -INFRAIA iNEXT-Discovery - Structural Biology Research Infrastructures for Translational Research and Discovery (contract n° 871037), EOSC-Life "Providing an open collaborative space for digital biology in Europe" (H2020, contract n° 824087), and "RNAct" Marie Sklodowska-Curie Action (MSCA) Innovative Training Networks (ITN) H2020-MSCA-ITN-

2018 (contract n° 813239). The authors also acknowledge Mestrelab Research for providing Mnova software and Bruker BioSpin for AssureNMR software.

REFERENCES

(1) Gaharwar, A. K.; Singh, I.; Khademhosseini, A. *Nat. Rev. Mater.* **2020**, *5*, 686−705.
(2) Gu, L.; Mooney, D. J. *Nat. Rev. Cancer* **2016**, *16*, 56−66.
(3) Suri, S.; Han, L.-H.; Zhang, W.; Singh, A.; Chen, S.; Schmidt, C. E. *Biomed. Microdevices* **2011**, *13*, 983−993.
(4) Noh, I.; Kim, N.; Tran, H. N.; Lee, J.; Lee, C. *Biomater. Res.* **2019**, *23*, 3.
(5) Wei, Y.-T.; He, Y.; Xu, C.-L.; Wang, Y.; Liu, B.-F.; Wang, X.-M.; Sun, X.-D.; Cui, F.-Z.; Xu, Q.-Y. *J. Biomed. Mater. Res. B Appl. Biomater.* **2010**, *95B*, 110−117.
(6) Antich, C.; de Vicente, J.; Jiménez, G.; Chocarro, C.; Carrillo, E.; Montañez, E.; Gálvez-Martín, P.; Marchal, J. A. *Acta Biomater.* **2020**, *106*, 114−123.
(7) Skardal, A.; Zhang, J.; Prestwich, G. D. *Biomaterials* **2010**, *31*, 6173−6181.
(8) Chung, J. H. Y.; Naficy, S.; Yue, Z.; Kapsa, R.; Quigley, A.; Moulton, S. E.; Wallace, G. G. *Biomater. Sci.* **2013**, *1*, 763−773.
(9) Wu, Z.; Su, X.; Xu, Y.; Kong, B.; Sun, W.; Mi, S. *Sci. Rep.* **2016**, *6*, 24474.
(10) Poldervaart, M. T.; Wang, H.; van der Stok, J.; Weinans, H.; Leeuwenburgh, S. C. G.; Öner, F. C.; Dhert, W. J. A.; Alblas, J. *PLoS One* **2013**, *8*, No. e72610.
(11) Duan, B.; Hockaday, L. A.; Kang, K. H.; Butcher, J. T. *J. Biomed. Mater. Res. A* **2013**, *101A*, 1255−1264.
(12) Giuseppe, M. D.; Law, N.; Webb, B.; Macrae, R. A.; Liew, L. J.; Sercombe, T. B.; Dilley, R. J.; Doyle, B. J. *J. Mech. Behav. Biomed. Mater.* **2018**, *79*, 150−157.
(13) Jia, W.; Gungor-Ozkerim, P. S.; Zhang, Y. S.; Yue, K.; Zhu, K.; Liu, W.; Pi, Q.; Byambaa, B.; Dokmeci, M. R.; Shin, S. R.; Khademhosseini, A. *Biomaterials* **2016**, *106*, 58−68.
(14) Buwalda, S. J.; Vermonden, T.; Hennink, W. E. *Biomacromolecules* **2017**, *18*, 316−330.
(15) Chen, J.; Ouyang, J.; Chen, Q.; Deng, C.; Meng, F.; Zhang, J.; Cheng, R.; Lan, Q.; Zhong, Z. *ACS Appl. Mater. Interfaces* **2017**, *9*, 24140−24147.
(16) Zhu, Q.; Chen, X.; Xu, X.; Zhang, Y.; Zhang, C.; Mo, R. *Adv. Funct. Mater.* **2018**, *28*, No. 1707371.
(17) Wawrzyńska, E.; Kubies, D. *Physiol. Res.* **2018**, S319−S334.
(18) Iqbal, S.; Blenner, M.; Alexander-Bryant, A.; Larsen, J. *Biomacromolecules* **2020**, *21*, 1327−1350.
(19) Shigemitsu, H.; Kubota, R.; Nakamura, K.; Matsuzaki, T.; Minami, S.; Aoyama, T.; Urayama, K.; Hamachi, I. *Nat. Commun.* **2020**, *11*, 3859.
(20) Lau, C. M. L.; Jahanmir, G.; Yu, Y.; Chau, Y. *J. Controlled Release* **2021**, *335*, 75−85.
(21) Tae, H.; Lee, S.; Ki, C. S. *J. Ind. Eng. Chem.* **2019**, *75*, 69−76.
(22) Chang, D.; Park, K.; Famili, A. *Drug Discovery Today* **2019**, *24*, 1470−1482.
(23) Ziegler, C. E.; Graf, M.; Beck, S.; Goepferich, A. M. *Eur. Polym. J.* **2021**, *147*, No. 110286.
(24) Gombotz, W. R.; Wee, S. F. *Adv. Drug Delivery Rev.* **2012**, *64*, 194−205.
(25) Vermonden, T.; Censi, R.; Hennink, W. E. *Chem. Rev.* **2012**, *112*, 2853−2888.
(26) Kumar, S.; Koh, J. *Int. J. Mol. Sci.* **2012**, *13*, 6102−6116.
(27) Dong, A.; Jones, L. S.; Kerwin, B. A.; Krishnan, S.; Carpenter, J. F. *Anal. Biochem.* **2006**, *351*, 282−289.
(28) Kirkitadze, M.; Sinha, A.; Hu, J.; Williams, W.; Cates, G. *Procedia Vaccinol.* **2009**, *1*, 135−139.
(29) Arbogast, L. W.; Brinson, R. G.; Marino, J. P. *Anal. Chem.* **2015**, *87*, 3556−3561.
(30) Brinson, R. G.; Marino, J. P.; Delaglio, F.; Arbogast, L. W.; Evans, R. M.; Kearsley, A.; Gingras, G.; Ghasriani, H.; Aubin, Y.; Pierens, G. K.; Jia, X.; Mobli, M.; Grant, H. G.; Keizer, D. W.; Schweimer, K.; Ståhle, J.; Widmalm, G.; Zartler, E. R.; Lawrence, C. W.; Reardon, P. N.; Cort, J. R.; Xu, P.; Ni, F.; Yanaka, S.; Kato, K.; Parnham, S. R.; Tsao, D.; Blomgren, A.; Rundlöf, T.; Trieloff, N.; Schmieder, P.; Ross, A.; Skidmore, K.; Chen, K.; Keire, D.; Freedberg, D. I.; Suter-Stahel, T.; Wider, G.; Ilc, G.; Plavec, J.; Bradley, S. A.; Baldisseri, D. M.; Sforça, M. L.; de Zeri, A. C. M.; Wei, J. Y.; Szabo, C. M.; Amezcua, C. A.; Jordan, J. B.; Wikström, M. *mAbs* **2019**, *11*, 94−105.
(31) Jones, L. M.; Zhang, H.; Cui, W.; Kumar, S.; Sperry, J. B.; Carroll, J. A.; Gross, M. L. *J. Am. Soc. Mass Spectrom.* **2013**, *24*, 835−845.
(32) Pan, L. Y.; Salas-Solano, O.; Valliere-Douglass, J. F. *Anal. Chem.* **2014**, *86*, 2657−2664.
(33) Ehkirch, A.; Hernandez-Alba, O.; Colas, O.; Beck, A.; Guillarme, D.; Cianférani, S. *J. Chromatogr. B Analyt. Technol. Biomed. Life Sci.* **2018**, *1086*, 176−183.
(34) Brinson, R. G.; Ghasriani, H.; Hodgson, D. J.; Adams, K. M.; McEwen, I.; Freedberg, D. I.; Chen, K.; Keire, D. A.; Aubin, Y.; Marino, J. P. *J. Pharm. Biomed. Anal.* **2017**, *141*, 229−233.
(35) Ghasriani, H.; Hodgson, D. J.; Brinson, R. G.; McEwen, I.; Buhse, L. F.; Kozlowski, S.; Marino, J. P.; Aubin, Y.; Keire, D. A. *Nat. Biotechnol.* **2016**, *34*, 139−141.
(36) Arbogast, L. W.; Brinson, R. G.; Formolo, T.; Hoopes, J. T.; Marino, J. P. *Pharm. Res.* **2016**, *33*, 462−475.
(37) Arbogast, L. W.; Delaglio, F.; Tolman, J. R.; Marino, J. P. *J. Biomol. NMR* **2018**, *72*, 149−161.
(38) Arbogast, L. W.; Delaglio, F.; Brinson, R. G.; Marino, J. P. *Curr. Protoc. Protein Sci.* **2020**, *100*, No. e105.
(39) Wu, K.; Luo, J.; Zeng, Q.; Dong, X.; Chen, J.; Zhan, C.; Chen, Z.; Lin, Y. *Anal. Chem.* **2021**, *93*, 1377−1382.
(40) Pastore, A.; Salvadori, S.; Temussi, P. A. *J. Pept. Sci.* **2007**, *13*, 342−347.
(41) Sass, H.-J.; Musco, G.; Stahl, S. J.; Wingfield, P. T.; Grzesiek, S. *J. Biomol. NMR* **2000**, *18*, 303−309.
(42) Barrientos, L. G.; Dolan, C.; Gronenborn, A. M. *J. Biomol. NMR* **2000**, *16*, 329−337.
(43) Tycko, R.; Blanco, F. J.; Ishii, Y. *J. Am. Chem. Soc.* **2000**, *122*, 9340−9341.
(44) Lecoq, L.; Fogeron, M.-L.; Meier, B. H.; Nassal, M.; Böckmann, A. Solid-State NMR for Studying the Structure and Dynamics of Viral Assemblies. *Viruses* **2020**, *12* (), DOI: 10.3390/v12101069.
(45) Wiegand, T.; Lacabanne, D.; Torosyan, A.; Boudet, J.; Cadalbert, R.; Allain, F. H.-T.; Meier, B. H.; Böckmann, A. *Front. Mol. Biosci.* **2020**, *7*, 17.
(46) Hassan, A.; Quinn, C. M.; Struppe, J.; Sergeyev, I. V.; Zhang, C.; Guo, C.; Runge, B.; Theint, T.; Dao, H. H.; Jaroniec, C. P.; Berbon, M.; Lends, A.; Habenstein, B.; Loquet, A.; Kuemmerle, R.; Perrone, B.; Gronenborn, A. M.; Polenova, T. *J. Magn. Reson.* **2020**, *311*, No. 106680.
(47) Lu, M.; Russell, R. W.; Bryer, A. J.; Quinn, C. M.; Hou, G.; Zhang, H.; Schwieters, C. D.; Perilla, J. R.; Gronenborn, A. M.; Polenova, T. *Nat. Struct. Mol. Biol.* **2020**, *27*, 863−869.
(48) Eddy, M. T.; Yu, T.-Y.; Wagner, G.; Griffin, R. G. *J. Biomol. NMR* **2019**, *73*, 451−460.
(49) Gupta, R.; Zhang, H.; Lu, M.; Hou, G.; Caporini, M.; Rosay, M.; Maas, W.; Struppe, J.; Ahn, J.; Byeon, I.-J. L.; Oschkinat, H.; Jaudzems, K.; Barbet-Massin, E.; Emsley, L.; Pintacuda, G.; Lesage, A.; Gronenborn, A. M.; Polenova, T. *J. Phys. Chem. B* **2019**, *123*, 5048−5058.
(50) le Paige, U. B.; Xiang, S.; Hendrix, M. M. R. M.; Zhang, Y.; Folkers, G. E.; Weingarth, M.; Bonvin, A. M. J. J.; Kutateladze, T. G.; Voets, I. K.; Baldus, M.; van Ingen, H. *Magn. Reson.* **2021**, *2*, 187−202.
(51) Mroue, K. H.; MacKinnon, N.; Xu, J.; Zhu, P.; McNerny, E.; Kohn, D. H.; Morris, M. D.; Ramamoorthy, A. *J. Phys. Chem. B* **2012**, *116*, 11656−11661.

https://doi.org/10.1021/acs.analchem.1c01850
Anal. Chem. 2021, 93, 11208−11214

(52) Azaïs, T.; Von Euw, S.; Ajili, W.; Auzoux-Bordenave, S.; Bertani, P.; Gajan, D.; Emsley, L.; Nassif, N.; Lesage, A. *Solid State Nucl. Magn. Reson.* **2019**, *102*, 2−11.
(53) Cerofolini, L.; Giuntini, S.; Louka, A.; Ravera, E.; Fragai, M.; Luchinat, C. *J. Phys. Chem. B* **2017**, *121*, 8094−8101.
(54) Louka, A.; Matlahov, I.; Giuntini, S.; Cerofolini, L.; Cavallo, A.; Pillozzi, S.; Ravera, E.; Fragai, M.; Arcangeli, A.; Ramamoorthy, A.; Goobes, G.; Luchinat, C. *Phys. Chem. Chem. Phys.* **2018**, *20*, 12719−12726.
(55) Ravera, E.; Cerofolini, L.; Martelli, T.; Louka, A.; Fragai, M.; Luchinat, C. *Sci. Rep.* **2016**, *6*, 27851.
(56) Martelli, T.; Ravera, E.; Louka, A.; Cerofolini, L.; Hafner, M.; Fragai, M.; Becker, C. F. W.; Luchinat, C. *Chemistry* **2016**, *22*, 425−432.
(57) Fragai, M.; Luchinat, C.; Martelli, T.; Ravera, E.; Sagi, I.; Solomonov, I.; Udi, Y. *Chem. Commun.* **2014**, *50*, 421−423.
(58) Ravera, E.; Schubeis, T.; Martelli, T.; Fragai, M.; Parigi, G.; Luchinat, C. *J. Magn. Reson.* **2015**, *253*, 60−70.
(59) Cerofolini, L.; Giuntini, S.; Carlon, A.; Ravera, E.; Calderone, V.; Fragai, M.; Parigi, G.; Luchinat, C. *Chem. − Eur. J.* **2019**, *25*, 1984−1991.
(60) Cerofolini, L.; Fragai, M.; Ravera, E.; Diebolder, C. A.; Renault, L.; Calderone, V. *Biomolecules* **2019**, *9*, 370.
(61) Giuntini, S.; Balducci, E.; Cerofolini, L.; Ravera, E.; Fragai, M.; Berti, F.; Luchinat, C. *Angew. Chem., Int. Ed.* **2017**, *56*, 14997−15001.
(62) Ravera, E.; Ciambellotti, S.; Cerofolini, L.; Martelli, T.; Kozyreva, T.; Bernacchioni, C.; Giuntini, S.; Fragai, M.; Turano, P.; Luchinat, C. *Angew. Chem. Int. Ed. Engl.* **2016**, *55*, 2446−2449.
(63) Giuntini, S.; Cerofolini, L.; Ravera, E.; Fragai, M.; Luchinat, C. *Sci. Rep.* **2017**, *7*, 17934.
(64) Cerofolini, L.; Giuntini, S.; Ravera, E.; Luchinat, C.; Berti, F.; Fragai, M. *npj Vaccines* **2019**, *4*, 20.
(65) Viger-Gravel, J.; Paruzzo, F. M.; Cazaux, C.; Jabbour, R.; Leleu, A.; Canini, F.; Florian, P.; Ronzon, F.; Gajan, D.; Lesage, A. *Chemistry* **2020**, *26*, 8976−8982.
(66) Jaudzems, K.; Kirsteina, A.; Schubeis, T.; Casano, G.; Ouari, O.; Bogans, J.; Kazaks, A.; Tars, K.; Lesage, A.; Pintacuda, G. *Angew. Chem. Int. Ed. Engl.* **2021**, *60*, 12847.
(67) Wang, H.; Wang, L.; Li, C.; Wuxiao, Z.; Chen, G.; Luo, W.; Lu, Y. *Oncologist* **2020**, *25*, e1725−e1731.
(68) Herbert, J.; Wilcox, J. N.; Pham, K.-T. C.; Fremeau, R. T.; Zeviani, M.; Dwork, A.; Soprano, D. R.; Makover, A.; Goodman, D. S.; Zimmerman, E. A.; Roberts, J. L.; Schon, E. A. *Neurology* **1986**, *36*, 900−900.
(69) Hamilton, J. A.; Benson, M. D. *Cell. Mol. Life Sci.* **2001**, *58*, 1491−1521.
(70) Connors, L. H.; Lim, A.; Prokaeva, T.; Roskens, V. A.; Costello, C. E. *Amyloid* **2003**, *10*, 160−184.
(71) Walker, K. W.; Foltz, I. N.; Wang, T.; Salimi-Moosavi, H.; Bailis, J. M.; Lee, F.; An, P.; Smith, S.; Bruno, R.; Wang, Z. *J. Biol. Chem.* **2020**, *295*, 10446−10455.
(72) Fragai, M.; Luchinat, C.; Parigi, G.; Ravera, E. *J. Biomol. NMR* **2013**, *57*, 155−166.
(73) Sarker, B.; Papageorgiou, D. G.; Silva, R.; Zehnder, T.; Gul-E-Noor, F.; Bertmer, M.; Kaschta, J.; Chrissafis, K.; Detsch, R.; Boccaccini, A. R. *J. Mater. Chem. B* **2014**, *2*, 1470−1482.
(74) Wang, Q.-Q.; Liu, Y.; Zhang, C.-J.; Zhang, C.; Zhu, P. *Mater. Sci. Eng. C Mater. Biol. Appl.* **2019**, *99*, 1469−1476.
(75) Schuetz, A.; Wasmer, C.; Habenstein, B.; Verel, R.; Greenwald, J.; Riek, R.; Böckmann, A.; Meier, B. H. *ChemBioChem* **2010**, *11*, 1543−1551.
(76) Lu, X.; Guo, C.; Hou, G.; Polenova, T. *J. Biomol. NMR* **2015**, *61*, 7−20.
(77) Keller, R. The Computer Aided Resonance Assignment Tutorial (CARA); *The CARA/Lua Programmers Manual. DATONAL AG.*; CANTINA Verlag: Goldau. Switzerland, 2004.
(78) Leach, J. B.; Schmidt, C. E. *Biomaterials* **2005**, *26*, 125−135.
(79) Jia, J.; Richards, D. J.; Pollard, S.; Tan, Y.; Rodriguez, J.; Visconti, R. P.; Trusk, T. C.; Yost, M. J.; Yao, H.; Markwald, R. R.; Mei, Y. *Acta Biomater.* **2014**, *10*, 4323−4331.
(80) Ouyang, L.; Yao, R.; Zhao, Y.; Sun, W. *Biofabrication* **2016**, *8*, No. 035020.
(81) Gao, T.; Gillispie, G. J.; Copus, J. S.; Pr, A. K.; Seol, Y.-J.; Atala, A.; Yoo, J. J.; Lee, S. J. *Biofabrication* **2018**, *10*, No. 034106.
(82) Liao, Y.-H.; Jones, S. A.; Forbes, B.; Martin, G. P.; Brown, M. B. *Drug Delivery* **2005**, *12*, 327−342.

https://doi.org/10.1021/acs.analchem.1c01850
Anal. Chem. 2021, 93, 11208−11214